

A 120 mm Bore Quadrupole for the Phase I LHC Upgrade

P. Fessia, P. Granieri, F. Borgnolutti, F. Regis, D. Richter, and E. Todesco

Abstract—The phase I LHC upgrade foresees the installation of a new final focusing for the high luminosity experiences in order to be able to focus the beams in the interaction points to $\beta^* \sim 0.25$ cm. Key element of this upgrade is a large bore (120 mm) superconducting quadrupole. This article proposes a magnet design that will make use of the LHC main dipole superconducting cable. Due to the schedule constraints and to the budget restrictions, it is mandatory to integrate in the design the maximum number of features successfully used during the LHC construction. This paper presents this design option and the rationales behind the several technical choices.

Index Terms—Accelerator magnets.

I. INTRODUCTION

THE phase I upgrade [1], [2] of the interaction regions around the CMS and ATLAS experimental areas requires the replacement of the triplet, presently made by the MQXA [3] and MQXB [4] 70 mm aperture quadrupoles built by the US-Japan collaboration, with a new quadrupole MQXC, using the same Nb-Ti technology. This set of quadrupoles should have a larger aperture and longer length, thus allowing to squeeze β^* in the two interaction points up to 25-30 cm. The present lay-out of the optics is being finalized, and an aperture of 120 mm has been selected during an internal review of the project in July 2008 [2]. This corresponds to a cold mass length of the order of 8-10 m and an operational gradient of about 120 T/m at 1.9 K. It is foreseen to use the existing spare cable of the main LHC dipoles (both 01 and 02 cable types [5]) to cope with the tight schedule and to reduce the costs. The present paper presents a possible design that tries to make the maximum use of the experience, tooling and spare material gathered during the production of the long superconducting magnets for the LHC (CERN). The only novel feature of the design is a new cable insulation scheme that should allow the helium to better penetrate between strands. In this document we will review the choice of a new insulation scheme, the process that has led to identify the conductor distribution and to fix the collar width (analysis

Manuscript received October 18, 2009. First published March 25, 2010; current version published May 28, 2010. This project was supported by the European Community's Seventh Framework Programme (FP7/2007-2013) under Grant 212114.

P. Fessia, F. Borgnolutti, F. Regis, D. Richter, and E. Todesco are with the European Organization for the Nuclear Research (CERN), 1211 Geneva 23, Switzerland (e-mail: Paolo.Fessia@cern.ch).

P. Granieri is with European Organization for the Nuclear Research (CERN), 1211 Geneva 23, Switzerland, and also with the Ecole Polytechnique Federale de Lausanne (EPFL), Lausanne, Switzerland.

Color versions of one or more of the figures in this paper are available online at <http://ieeexplore.ieee.org>.

Digital Object Identifier 10.1109/TASC.2010.2043658

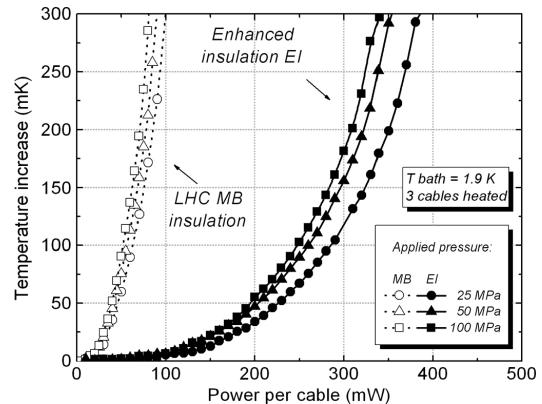


Fig. 1. Increase of the cable core temperature in function of the power dissipated in the cable for the LHC MB insulation and the new enhanced insulation scheme. Measurements at different compressive loads.

performed at room temperature, 1.9 K and 1.9 K with Lorentz forces).

In the end a brief section will provide estimates of the possible field errors.

II. CABLE INSULATION

The increase of luminosity put a further requirement on the coils to cope with an increased heat deposition [2]. In order to improve the coil transparency to helium a new insulation scheme has been proposed and is being tested [6], [7]. The new insulation provides enhanced heat transfer capacity with respect to the standard LHC insulation through channels that are created between the three polyimide layers. This improved heat transfer is not depleted by the coil compression status as shown in Fig. 1. The measured insulation thickness is radially 0.16 mm and azimuthally 0.135 mm for the cable type 01 (inner layer) and 0.145 mm for the cable type 02 (outer layer).

III. CROSS SECTION CHOICE

The semi-analytical scaling laws developed in [8] allow estimating the short sample gradient of ironless quadrupoles as a function of the magnet aperture, of the coil width and of the superconducting cable short sample current. Applying such scaling law for a 120 mm quadrupole aperture, without grading and iron, with a Nb-Ti conductor similar to the LHC MB inner cable, a one layer coil would give a short sample gradient of about 110 T/m. Adding a second layer, 140 T/m can be reached, and a third layer would provide 150 T/m. From this estimate, the increase of about 7% obtained by adding a third layer seems not an interesting gain and a two-layer coil looks

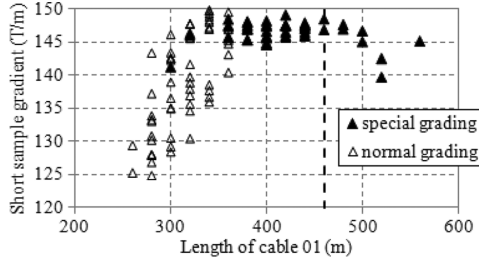


Fig. 2. Short sample gradient versus the length of the cable 01 needed to wind one pole (head excluded) for the normal grading (empty markers) and for the special grading (full marker). The dotted line is the available cable unit length.

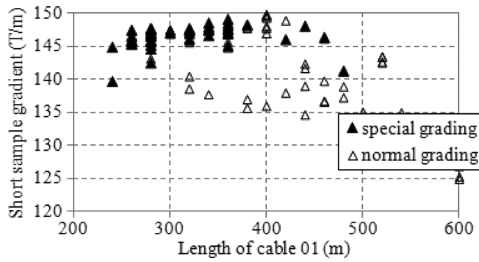


Fig. 3. Short sample gradient versus the length of the cable 02 needed to wind one pole (head excluded) for the normal grading case (empty markers) and for the special grading case (full marker).

as a good compromise in having a large gradient limiting the use of the cable from the LHC spares.

To optimize the three multipoles (b_6 , b_{10} and b_{14}) and the gradient it was decided to focus on the use of a four-block coil, as adopted as the LHC MQ [9] or MQXB; this provides 6 angles as free parameters. The space of the possible cross sections, fulfilling the requirements $|b_6| < 1$, $|b_{10}| < 0.5$ and $|b_{14}| < 0.2$ units, has been explored as a function of the quantity of cable to be used and of the resulting quench gradient [10]. Special grading solutions, where 01 cable is used in the outer layer upper block, have been also taken into consideration. The results are shown in Figs. 2 and 3:

- The largest short sample gradient is around 150 T/m, to be compared to the previous estimate of 140 T/m, which neglected both the iron and the grading effect.
- Both special grading and normal grading have similar maximal gradients (within 1%).
- There are a large number of solutions with special grading using much more cable 01 than the available unit lengths of 480 m: these are not therefore fulfilling our requirements.

The engineering constraints are the following:

- The inner layer arch length of the pole spacer should be at least 18 mm to guarantee a good winding stability (according to previous experience with LHC 01 cable)
- The quench current should be less than 16 KA in order to have a nominal working point (fixed by the project at 80% of the quench current) in the range of the LHC known power converters set ups.
- The design should integrate a midplane insulation of at least 0.225 mm in order to provide 0.1 mm as field quality tuning shim if needed.

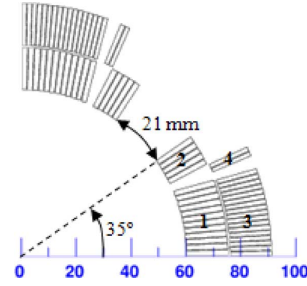


Fig. 4. Proposed cross section of the MQXC magnet. The block numbering is indicated.

TABLE I
GEOMETRIC PARAMETERS OF THE COIL

Block N°	Nb. Cond.	r (mm)	ϕ (°)	γ (°)	cable type
1	12	60.00	0.21	0.00	cable 01
2	5	60.00	25.73	27.76	cable 01
3	17	75.92	0.15	0.00	cable 02
4	2	75.92	23.50	22.76	cable 02

TABLE II
MAIN FEATURES OF MQXC (1.9 K)

	unit	MQXC
Aperture diameter	mm	120
Inner iron diameter	mm	260
Outer iron diameter	mm	550
Short sample Gradient	T/m	147.1
Short sample current	kA	15.9
Nominal gradient	T/m	118.5
Nominal current [In]	kA	12.72
Inductance	mH/m	5.06
Reference radius	mm	40
Fx (I = In)	MN/m	0.93
Fy (I = In)	MN/m	-1.35

Taking into account the previous boundary conditions, the cross section in Fig. 4 is proposed. Its geometrical features and characteristics are listed in Tables I and II.

IV. MECHANICAL CONSIDERATIONS

It was decided to explore the possibility to use a self standing collar structure that would allow decoupling the collar coil mechanics from the cold mass assembly. In order to get a first estimate of the collar thickness needed for the self standing option approximation it has been decided to limit the coil deformation as in the LHC MQXB. In Fig. 5 is shown the collar thickness versus aperture radius and versus the number of coil layers [11]. For an aperture of 120 mm diameter, this simplified analytic model indicates a collar thickness of 39 mm indicating also that the choice of 3 layers would have brought to collar thickness to more than 50 mm for only $\sim 7\%$ more gradient. It has been then decided to limit the coil radial deformation on the midplane to 60 μm and to cross check through a finite element model.

Fig. 6 indicates that a 35 mm steel collar fulfills the requirement. Fig. 7 shows instead the difference in azimuthal stress

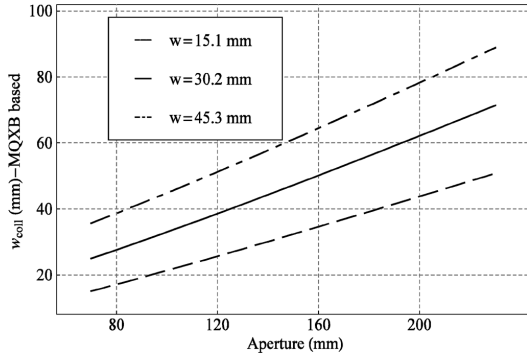


Fig. 5. Collar thickness for cross sections with 1, 2, 3 layers (w represents the insulated cable width). The thickness is such to obtain the same deformation due to magnetic forces as for the MQXB, at I_{SS} .

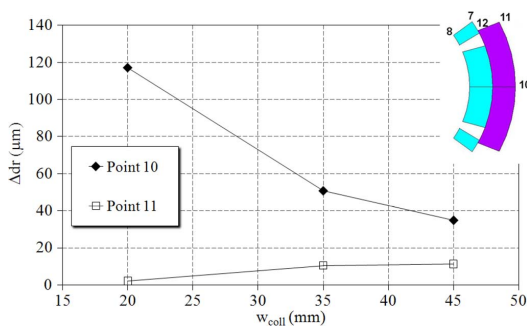


Fig. 6. Coil deformation due to magnetic forces in point 10 and 11 in function of the used collar thickness.

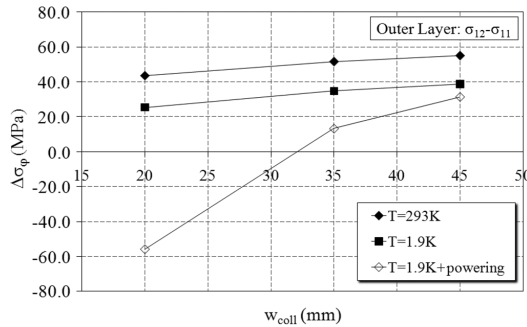


Fig. 7. Variation of the difference in azimuthal stresses between the outer layer upper edges in function of the collar thickness.

$\Delta\sigma_\phi$ between the inner and outer pole edges of the outer layer. This difference is related to the stiffness of the collar pack: at powering $\Delta\sigma_\phi$ approaches the value observed after cool down, as long as the collar thickness is increased. The difference in stress $\Delta\sigma_\phi$ is less and less relevant for $w_{coll} > 35$ mm, which is therefore taken as design value for the collar thickness. The same behavior is observable on the computed stress difference for the inner layer and indicates a reduction of the deformation due to the bending moment in function of the increased collar stiffness.

V. IRON YOKE AND TRANSFER FUNCTION

Taking into account a 2-mm-gap between collars and the iron yoke, the inner diameter of the iron is set at 260 mm. Its outer diameter is at 550 mm for tooling (LHC MBouter diameter) and tunnel transport constraints. Two possible configurations

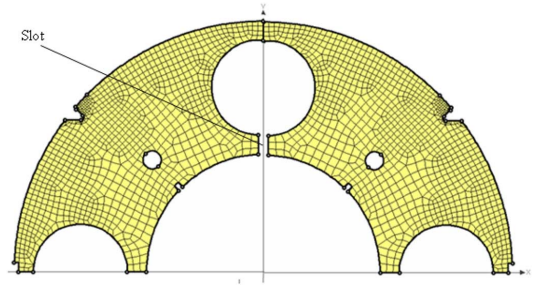


Fig. 8. Iron yoke design (upper half shown) with hole for the heat exchanger on the vertical midplane and slot for helium transparency.

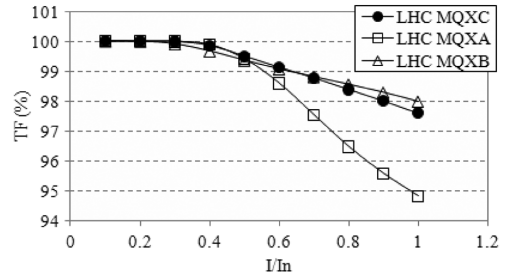


Fig. 9. Transfer functions of the MQXC with respect to the LHC MQXA and LHC MQXB.

for the heat exchanger have been studied: the first configuration needs two 80 mm diameter exchangers, and the second one needs one 105 mm diameter exchanger. The yoke must anyway have four holes to satisfy the four-fold symmetry of the magnet, thus avoiding unallowed multipoles. Two angular positions are possible on the midplane or at 45° (see Fig. 8).

From the tunnel integration point of view, the best choice would be to use only one exchanger on the vertical midplane providing full symmetry between the different installation points and minimizing the interconnect work. Taking into account four holes of 105 mm in line with the midplane, the reduction of the transfer function at nominal current, due to the iron saturation with the holes, is $\sim 2.5\%$, in between what we have for the LHC MQXA (6%) and MQXB (2%) (Fig. 9) and it is therefore probably acceptable.

The impact on b_6 is 1-2 units while on b_{10} and b_{14} is within 0.1 units. Recently [12] it has been shown a larger impact on the field quality when the holes are positioned on the mid plane and the vertical misalignment of the cryostat is taken into consideration. This effect could bring to move the heat exchanger at 45 degrees or to introduce iron feature to counter-compensate it. The introduction of a slot joining the heat exchanger cavity to the collared coil cavity has been studied. The effect of this slot has been evaluated in a variation of 0.06 unit of b_4 and -0.04 unit of b_6 and therefore could be an interesting solution to increase the yoke helium transparency if needed.

VI. END DESIGN

The objective of the end design was to limit the peak field in the ends and subsidiary to reduce as much as possible their impact on the global filed error content. The attempt to keep full iron all over the ends was made. The proposed cable distribution for the non connection side end is shown in Fig. 10. At nominal current the peak field seen by the cable 01 is 7.9 T in the straight

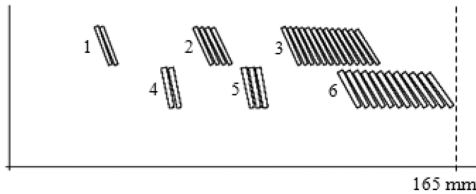


Fig. 10 Proposed cable distribution for the non connection side end.

 TABLE III
MULTIPOLE CONTENT

	Lmag[mm]	b ₆	b ₁₀	b ₁₄	a ₆	a ₁₀	a ₁₄
Straight part	7250	-0.01	-0.03	-0.07	0.0	0.0	0.0
Layer jump	240	0.4	-0.08	0.0	-0.2	-0.02	0.01
Heads	226	-0.2	-0.15	-0.02	0.0	0.0	0.0
Total	7716	0.19	-0.26	-0.09	-0.2	-0.02	0.01

part and increase to 8 T in the head. This is equivalent to 81% of the short sample. In this design, with iron covering the heads, the peak field in the head is about 1% larger than in the straight part; this increase has not been judged as critical. For the cable outer layer the peak field in the straight part is lower, 6.6 T, and it increases to 7 T in the head again to the 81% of the short sample for the cable 02. The head physical length is 165 mm with an equivalent magnetic length of 113 mm. The average multipole over this length are $b_6 = -6.5$ $b_{10} = -5.5$ and $b_{14} = -0.4$ units.

VII. FIELD QUALITY

Table III reports the field quality for a magnet with a straight part of 7250 mm that is up today the shortest possible optic solution. Please note that for the moment the contribution of two non connection side heads are accounted not having the data for the connection side.

Concerning the field errors, estimations of the uncertainty and of the random are provided in Table IV. The uncertainty is computed from the combination of the following possible defects that have been singularly evaluated [13]:

- 1) Yoke ellipticity ± 0.1 mm
- 2) Coil misplaced with respect to the yoke ± 0.1 mm
- 3) Collar cavity radius ± 0.05 mm
- 4) Defect on the collar nose thickness ± 0.05 mm
- 5) Defect on the collar permeability $\mu_r = 1.003$
- 6) Error on the azimuthal thickness of the copper wedges ± 0.05 mm
- 7) Error on the keystone angle of the copper wedges ± 0.05 mm
- 8) Collars deformation during powering 0.05 mm
- 9) Defect in curing mould ± 0.05 mm

 TABLE IV
FIELD ERROR TABLE

	b3	b4	b5	b6	b7	b8	b9	b10
Uncertainty	0.46	0.64	0.46	1.77	0.21	0.16	0.08	0.2
Random	0.89	0.64	0.46	1.28	0.21	0.16	0.08	0.06
	a3	a4	a5	a6	a7	a8	a9	a10
Uncertainty	0.89	0.64	0.46	1.27	0.21	0.16	0.08	0.14
Random	0.89	0.64	0.46	0.33	0.21	0.16	0.08	0.06

The random components have been derived from the analysis of the coil mispositioning of the LHC magnets of type MQ, MQY, MQXA, MQXB. As result a value of 0.03 mm at 1σ has been assumed [14].

VIII. CONCLUSION

A design for a 120 mm 120 T/m quadrupole has been proposed trying to integrate at maximum components and material availability, assembly and tunnel integration constraints. The present solution can be considered as a starting point for a detailed design based on these principles. The design is described in detail in [13], [15].

REFERENCES

- [1] J. P. Koutchouk, L. Rossi, and E. Todesco, A Solution for Phase-One Upgrade of the LHC Low-Beta Quadrupoles Based on Nb-Ti LHC Project Report 1000, 2007.
- [2] R. Ostojic *et al.*, Conceptual Design of the LHC Interaction Region Upgrade: Phase-I LHC PROJECT Report 1163, 2008.
- [3] Y. Ajima *et al.*, *Nucl. Instrum. Meth. A*, vol. 550, p. 499, 2005.
- [4] M. Lamn *et al.*, in *European Particle Accelerator Conference 2637*, 2006.
- [5] LHC Project Report Cable Data.
- [6] P. Fessia *et al.*, "Electrical and mechanical performance of an enhanced cable insulation scheme for the superconducting magnets of the LHC luminosity upgrade," *IEEE Trans. Appl. Supercond.*, submitted for publication.
- [7] P. Granieri *et al.*, "Heat transfer of an enhanced cable insulation scheme for the superconducting magnets of the LHC luminosity upgrade," *IEEE Trans. Appl. Supercond.*, submitted for publication.
- [8] L. Rossi and E. Todesco, *Phys. Rev. STAB*, vol. 9, p. 102401, 2006.
- [9] O. Bruning, LHC Design Report vol. I.
- [10] F. Borgnolutti, "A method for coil design of superconducting quadrupoles based on sector coils and Fourier transform," *IEEE Trans. Appl. Supercond.*, submitted for publication.
- [11] P. Fessia, F. Regis, and E. Todesco, "Parametric analysis of forces and stresses in superconducting quadrupole sector windings," *IEEE Trans. Appl. Supercond.*, vol. 17, pt. 2, pp. 1269–1272, Jun. 2007.
- [12] S. Russenschuck, presented at the TDG Weekly Meeting CERN, Geneva, Switzerland.
- [13] F. Borgnolutti, P. Fessia, and E. Todesco, Electromagnetic Design of the 120 mm Aperture Quadrupole for the LHC Phase One Upgrade CERN, sLHC-PROJECT-Report-0001, 2009.
- [14] B. Bellesia, C. Santoni, and E. Todesco, "Random errors in superconducting dipoles," in *10th European Particle Accelerator Conference*, Edinburgh, UK, Jun. 26–30, 2006, p. 2601.
- [15] P. Fessia and F. Regis, LHC Upgrade Phase I: Preliminary Study of the Collar Structure for the New Inner Triplet Quadrupole CERN, sLHC-PROJECT-Report-0002, 2009.